

Residue Cover and Surface-Sealing Effects on Infiltration: Numerical Simulations for Field Applications

Huanxiang Ruan,* Laj R. Ahuja, Timothy R. Green, and Joseph G. Benjamin

ABSTRACT

Surface sealing of bare soils often reduces rain infiltration, and crop-residue cover is commonly used to reduce surface sealing. We conducted numerical experiments to quantify effects of the percentage and distribution of residue cover on infiltration, and to provide guidelines for residue management. Residue cover was simulated over the soil surface in circular patches. Excess surface water from the bare surface-sealed areas was available for infiltration in nonsealed areas. Numerical simulations were conducted for combinations of (i) soil type, either a clay loam or loamy sand soil; (ii) percentage residue cover (P_r); (iii) saturated hydraulic conductivity of the surface seal (K_s) relative to bulk soil (K_b); (iv) residue-patch size with a constant P_r ; and (v) rainfall intensity. The K_s values had the greatest influence on infiltration as a function of P_r . This influence increased with rainfall intensity. For a given P_r , smaller patches gave greater relative infiltration due to differences in the lateral redistribution of infiltrated water. The target values of P_r that provided 95% relative infiltration varied from 40 to 80% for most combinations. Changing the geometry of the residues made no significant difference. We also tested a one-dimensional model with a spatially averaged saturated hydraulic conductivity (K_a) for both covered and surface-sealed areas, and found that infiltration into a partially residue-covered soil could be estimated by the one-dimensional model for all cases of this study, when $K_s > 0$. Finally, simulated infiltration qualitatively agreed with data sets of two independent field experiments under similar soil and rainfall conditions.

WATER AVAILABILITY is a major factor in crop productivity in the vast arid and semiarid regions of the world. Water use efficiency, which is defined in terms of the proportion of total available water transpired by a crop, is critical in an era of increasing competition for water use. Practices that increase rain infiltration and minimize runoff are important to increase water use efficiency.

The impact of raindrops on a bare soil surface forms a thin layer known as a surface seal on the soil surface due to a combination of physical and chemical processes. The surface seal is denser and has a lower saturated hydraulic conductivity than that of the bulk soil (Tackett and Pearson, 1965). Water infiltration into the bare soil is most often determined by the surface seal (Duley, 1939; Ellison and Slater, 1945; McIntyre, 1958; Ahuja, 1974; Morin and Benyamini, 1977; Ahuja, 1983; Eigel and Moore, 1983; Smith et al., 1999). Crop residues protect the soil surface from physical raindrop impact, which can reduce the formation of surface seals and increase the infiltration rate (Unger and Stewart, 1983). On the other hand, rainfall interception by residue cover

may decrease infiltration (Savabi and Stott, 1994) and is an issue we do not consider in this study.

The relationship between the mass or extent of residue cover and the increase in infiltration is an important issue in dealing with the surface-sealing problem. Baumhardt and Lascano (1996) conducted a field experiment near Lubbock, TX. Simulated rain was applied at 65 mm h^{-1} for 1 h on a bare and residue-covered Olton clay loam soil. They found that cumulative infiltration was lowest (28.7 mm) on bare soil, and increased curvilinearly with increasing residue amounts, leveling off to a limit (49.0 mm). The leveling off (asymptotic limit) occurred at a residue amount of 2.4 ton ha^{-1} . Increases in infiltration were related to the residue amount and not influenced by residue geometry, or their location on the bed or furrow. Lang and Mallett (1984) compared six levels of maize stover, expressed as a percentage ground cover (0, 10, 20, 30, 45, and 75%) under a rainfall simulator (rainfall intensity of 63.5 mm h^{-1}) to assess the effect of surface residues on infiltration and soil loss on a clay loam soil with a 3.5% slope. The increase of infiltration was curvilinearly related to the ground-cover percentage, and the infiltration was 54% greater with 45% residue cover than without residue cover.

It would be extremely useful to know what level of residue cover would be adequate to achieve maximum infiltration, or perhaps 95% of the maximum. This infiltration would be especially important in arid and semiarid regions, where water is the most limiting factor for crop production. It is surprising that only a few studies have been conducted to quantify the residue-cover efficiency.

A number of modeling studies on infiltration into surface-sealed soils have been reported (e.g., Mualem and Assouline, 1989; Baumhardt et al., 1990). Without residues, surface seals are formed uniformly over the soil surface and the water infiltration and redistribution in soils are in one dimension, if the soil is otherwise homogeneous and flat. Several other studies have modeled the water infiltration into the surface-sealed or crusted soil using one-dimensional methods (Ahuja, 1973; Ahuja, 1983; Ahuja and Swartzendruber, 1992; Mualem et al., 1993; Philip, 1998; Smith et al., 1999). Most models such as the RZWQM (RZWQM Development Team, 1998) use one-dimensional approaches.

Infiltration into soil partially covered by crop residues is a two-dimensional problem for which we need to use a two-dimensional model. However, if we can determine an effective saturated hydraulic conductivity for the soil surface that allows the same amount of infiltration as

Huanxiang Ruan, Laj R. Ahuja, and Timothy R. Green, USDA-ARS-NPA, Great Plains Systems Research Unit, P.O. Box E, 301 S. Howes St., Fort Collins, CO 80522; Joseph G. Benjamin, USDA-ARS-NPA, Central Great Plains Research Unit, Akron, CO 80720. Received 15 Mar. 1999. *Corresponding author (ruan@gpsr.colostate.edu).

Abbreviations: P_r , percentage residue cover; K_s , saturated hydraulic conductivity of the surface seal; K_b , saturated hydraulic conductivity of bulk soil; K_a , spatially averaged saturated hydraulic conductivity; R_1 , radius of the residue patch; R_2 , radius of the cylinder.

an actually distributed surface seal, we could use one-dimensional methods instead of two-dimensional methods to simulate the infiltration. The effective saturated hydraulic conductivity for a nonuniform or patchy surface seal (K_{ce}) could be formulated with the saturated hydraulic conductivities of the surface seal and the non-sealed soil and the P_{rc} . For practical purposes, it would be very useful to evaluate this effective one-dimensional approach.

Objectives of this theoretical study were (i) to quantify rain infiltration in two typical soil textures (clay loam and loamy sand) as a function of percentage residue cover (residue-cover efficiency); (ii) to examine the sensitivity of residue-cover efficiency to the surface-seal hydraulic conductivity (K_c), the residue-patch size, and the rainfall intensity; and (iii) to evaluate the use of an effective saturated hydraulic conductivity of the nonuniform surface seal (K_{ce}) so that the infiltration can be simplified as a one-dimensional problem.

MATERIALS AND METHODS

Soil Parameters and Rainfall Intensities

Two soils of typical textures were used in this study. The first was an Ulm clay loam (fine, smectitic, mesic Ustic Haplargids) located at the Agricultural Research Demonstration and Education Center near Fort Collins, CO, and the second was a Crook loamy sand (mixed, mesic, Ustic, Torripsamment) as reported by Benjamin et al. (1994). Other than the surface seal, the soils were assumed homogeneous and isotropic. The hydraulic properties used for the numerical simulations are listed in Table 1 and were measured by Benjamin et al. (1994).

A surface seal was assumed to exist on the part of the bare soil surface that was not covered by residues. The surface seal was assumed to form quickly under rainfall, and thus was assumed to be saturated at time zero and to have a constant thickness. The saturated hydraulic conductivity of the surface seal (K_c) was selected at three levels: 0, 0.1, and 0.3 times the saturated hydraulic conductivity of the bulk soil (K_s). Actual values of K_c were expected to fall in the range from 0.05 K_s to 0.5 K_s (Rawls et al., 1990). We used 5 mm as the surface-seal thickness (after Baumhardt et al., 1990; Mualem et al., 1993).

As an upper boundary condition, we used rainfall intensities of 25 mm h⁻¹, 65 mm h⁻¹, or 250 mm h⁻¹ for a 1-h duration. The evaporation in this short time period was assumed to be negligible compared with the rainfall. The value 250 mm h⁻¹ was arbitrarily selected as an extreme limit. The rainfall intensity value of 25 mm h⁻¹, which was slightly greater than the saturated hydraulic conductivity of the clay loam soil, was selected because at lower rainfall intensities, all water will infiltrate. Similarly, the rainfall intensity value of 65 mm h⁻¹ was slightly greater than the K_s of the loamy sand soil. The rainfall intensity of 65 mm h⁻¹ was the same as the rainfall intensity that was used by Baumhardt and Lascano (1996) and

Table 1. Soil properties of clay loam and loamy sand (Benjamin et al., 1994).†

Soil type	K_s	θ_s	θ_r	α	n	β
	mm h ⁻¹	-	mm ³ mm ⁻³	mm ⁻¹		
Clay loam	17.2	0.39	0.10	0.0085	1.23	13
Loamy sand	61.1	0.37	0.04	0.0059	1.65	3

† K_s is saturated hydraulic conductivity, θ_s is saturated water content, θ_r is residual water content, α and n are coefficients for the van Genuchten water retention equation (Eq. [2]), and β is the power for the unsaturated hydraulic conductivity equation (Eq. [3]).

was only 1.5 mm h⁻¹ greater than that used by Lang and Mallett (1984). Both Baumhardt and Lascano (1996) and Lang and Mallett (1984) used a 1-h duration. These conditions allowed a better comparison of our research with theirs. At the bottom of the domain, the soil was assumed to be free-draining.

Residue-Patch Geometry

We assumed a flat soil condition and that the portion of the soil surface covered by residues had no surface seal. In nature, the residues and bare areas on the soil surface may be distributed in a variety of ways. To model infiltration into a soil that was partially residue-covered, we assumed two simplified geometrical distributions of residue cover. The first type (Type I) was a simple residue distribution (Fig. 1), that is, residues were in circular patches surrounded by concentric bare spaces. In this case, we could choose one residue patch, plus the concentric bare space, as the representative unit. The second type (Type II) was the same as the first, except that the circular bare spaces were surrounded by concentric residues. Another type of geometrical distribution of residue cover that we could have considered was residues placed in strips. We hope to simulate this special geometry of residue distribution in a future study.

The following descriptions are for residue geometry Type I. For residue geometry Type II, the changes should be straightforward. We calculated infiltration into the representative cylinder in which flow is symmetrical (Fig. 2) and can be solved using a two-dimensional method in the cylindrical coordinates (r , z). The radius of the residue patch is R_1 and the radius of the cylinder is R_2 . The depth, D , is 1000 mm. Residue is in the center and the surface seal is in the remaining area.

The residue-patch size may change with the P_{rc} in a variety of ways. For simplicity, we used two different methods to examine the effect of the residue-patch radius on the residue-cover efficiency: (i) residue-patch size does not change with P_{rc} , or (ii) residue-patch size changes with P_{rc} linearly. In method (i), R_1 was set to one of the three sizes (50, 100, and 200 mm), which we assumed to be the typical residue-patch sizes. To get different values of P_{rc} , which equal $(R_1/R_2)^2 \times 100\%$, we changed R_2 and kept R_1 constant once R_1 was selected. Here, $R_2 \geq 50, 100, \text{ or } 200$ mm. In method (ii), R_2 was set to one of the same three sizes as above (50, 100, or 200 mm), and P_{rc} was set to change with R_1 , once R_2 was selected. Here, $R_1 \leq 50, 100, \text{ or } 200$ mm.

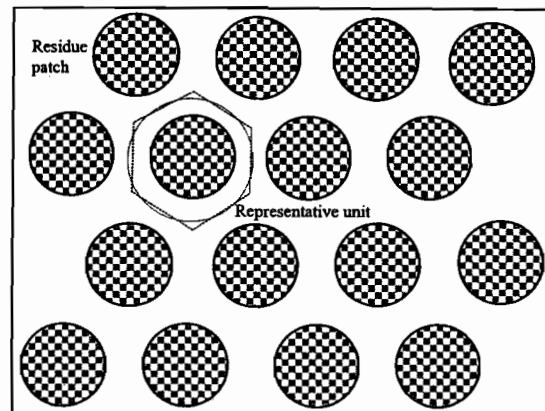


Fig. 1. For residue distribution Type I, uniform residue patches are distributed evenly. The representative unit is simplified from a hexahedron to a cylinder. For residue distribution Type II, the residue area is simply switched with the sealed area.

Two-Dimensional Infiltration and Redistribution Model

The governing equation is given by the following modified cylindrical form of Richards' equation (Bruggeman and Mos-taghimi, 1991):

$$\frac{d\theta}{dh} \left(\frac{\partial h}{\partial t} \right) = \left(\frac{1}{r} \right) \frac{\partial}{\partial r} \left(rK \frac{\partial h}{\partial r} \right) + \frac{\partial}{\partial z} \left[K \frac{\partial (h + z)}{\partial z} \right] \quad [1]$$

where θ is the water content, h is the hydraulic pressure head, and K is the hydraulic conductivity, which is a function of h or θ .

The relationship between θ and h is the key hydraulic property. Van Genuchten's model (van Genuchten, 1980) was used to relate these two hydraulic variables:

$$\theta(h) = \theta_r + (\theta_s - \theta_r) \left[\frac{1}{1 + (-\alpha h)^n} \right]^{(1-1/n)} \quad [2]$$

where θ_r is the residual water content, θ_s is the saturated water content, and α and n are the fitted parameters that control the shape of the $\theta(h)$ curve.

The hydraulic conductivity function we used is the equation presented by Corey (1994):

$$K(\theta) = K_s \left(\frac{\theta - \theta_r}{\theta_s - \theta_r} \right)^\beta \quad [3]$$

where K_s is the saturated hydraulic conductivity, and β is the parameter related to the soil type. We used Corey's equation instead of van Genuchten-Mualem's equation.

We used SWMS_2D (Simunek et al., 1994), a two-dimensional finite element model, to solve Eq. [1]. The surface boundary conditions of SWMS_2D were modified to deal with the surface seal. The boundary condition at $r = R_2$ was a zero flux boundary. The boundary at $z = D$ was a flux boundary that was equal to a unit hydraulic gradient multiplied by the hydraulic conductivity. In the residue-covered area, it was a flux boundary (rainfall plus run-on from the surface-sealed area) before runoff occurred and was a zero head boundary after runoff occurred (when the soil surface was saturated).

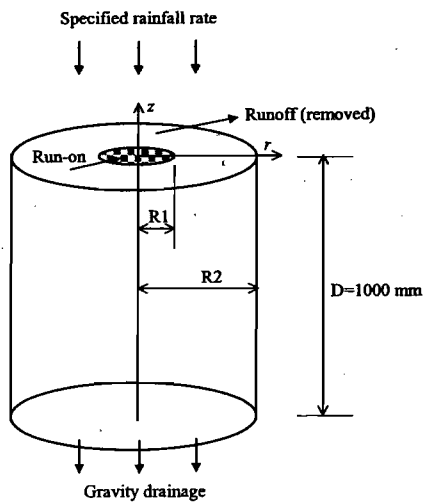


Fig. 2. Representative soil cylinder with residues in the center and surface seal in the remaining area (Type I). R_1 is the radius of the residue patch. R_2 is the radius of the soil cylinder. D is the depth of the soil cylinder. Water may first run on to a residue-covered area from a surface-sealed area. Excess water from both the residue-covered area and surface-sealed area then become runoff, which is removed from the system.

In the surface-sealed area, we separated the surface-seal layer from the flow domain of the finite element mesh. We assumed that the surface seal developed very rapidly after the start of rainfall or the seal existed before the infiltration event. As a result, the change of water content in the surface seal was negligible, and the surface-seal hydraulic conductivity was constant and equal to K_c (Ahuja, 1983). Mualem et al. (1993) also set the seal to be saturated at the very beginning of rainfall. We simplified the hydraulic pressure head within the surface seal to linearly change from the top to the bottom of the surface seal. At the top of the surface seal, the hydraulic pressure head was zero when there was excess rainwater and a negative value determined by the dynamics of the simulation when all rainfall water had infiltrated into the surface seal. At the bottom of the surface seal, the hydraulic pressure head was equal to the hydraulic pressure head of the soil below the surface seal.

The surface-seal layer controlled the flux at the soil surface that was the flux admitted to soil beneath the surface seal. This flux was used as the flux boundary condition in the surface-sealed area of the flow domain of the finite element mesh. To find the flux entering the surface seal, we set the pressure head at the top of the surface seal to zero and set the pressure head at the bottom of the surface seal to the pressure head of the previous time step at the boundary of the flow domain below the surface seal. The flux was then obtained using the hydraulic gradient and the saturated hydraulic conductivity of the surface seal (K_c). If the flux was less than the rainfall, the flux was used as the flux boundary condition in the surface-sealed area. If the flux was greater than the rainfall, the rainfall was used as the flux boundary condition in the surface-sealed area. Generally, the flux through the surface seal was controlled by the rainfall intensity in early stages (no ponding) and by the hydraulic gradient within the surface seal later (ponding).

When infiltration was controlled by the infiltration capacity (the hydraulic gradient multiplied by the saturated hydraulic conductivity of the surface seal), the excess rainwater from the surface-sealed area was instantaneously redistributed over the residue-covered area where the infiltration capacity was greater. When the excess water from the surface-sealed area, plus the rainwater directly applied on the residue-covered area, exceeded the infiltration capacity of the residue-covered area, runoff occurred. The runoff was removed instantaneously.

One-Dimensional Model Using an Effective Surface Seal

Water infiltration and redistribution in soils were simplified as a one-dimensional problem by assuming that a uniform effective surface seal covered the entire soil surface including residue-covered and uncovered areas. The effective surface seal had an effective saturated hydraulic conductivity (K_{ce}) and the same thickness as the surface seal in the surface-sealed areas. The value of K_{ce} must be greater than K_c of the surface-sealed areas and less than K_s of the residue-covered areas. A linear interpolation was a simple method to obtain K_{ce} :

$$K_{ce} = K_c(1 - P_{rc}) + K_s P_{rc} \quad [4]$$

where K_c is the saturated hydraulic conductivity of surface seal and K_s is the saturated hydraulic conductivity of the bulk soil. We used Eq. [4] to obtain the one-dimensional infiltration, although another function may be better than linear interpolation. All conditions other than K_c were the same as what were stated in the two-dimensional model.

RESULTS AND DISCUSSION

Total Number of Simulated Combinations (Two-Dimensional)

The total number of factor combinations that we simulated with the two-dimensional model was 2 (residue geometrical distribution) × 2 (soil) × 3 (surface-seal saturated hydraulic conductivity) × 3 (residue size) × 2 (the way residue size changed with P_{rc}) × 3 (rainfall intensity) = 216 (cases). For every combination of factors (cases), 11 values of P_{rc} (0, 4.7, 14.7, 26.7, 42.3, 51.4, 72.2, 84.0, 90.3, 96.7, and 100%) were selected to simulate the infiltration. The total number of simulations was 216 (cases) × 11 (P_{rc}) = 2376.

Cases with Simple Residue-Cover Efficiency

Model-simulated results of 96 cases (of 216 cases total) were outside the scope of surface-seal effects. With the combination of the loamy sand soil and a rainfall intensity of 25 mm h⁻¹ (36 cases), and the combination of the loamy sand soil, a rainfall intensity of 65 mm h⁻¹, and $K_c \geq 0.1K_s$ (24 cases), all rainwater infiltrated. When rainfall intensity was small relative to K_s , residue cover was not needed. With the combination of the clay loam soil and a rainfall intensity of 250 mm h⁻¹ (36 cases), the simulated infiltration was not significantly different from the infiltration at the rainfall intensity of 65 mm h⁻¹. This was because residue cover can, at most, prevent

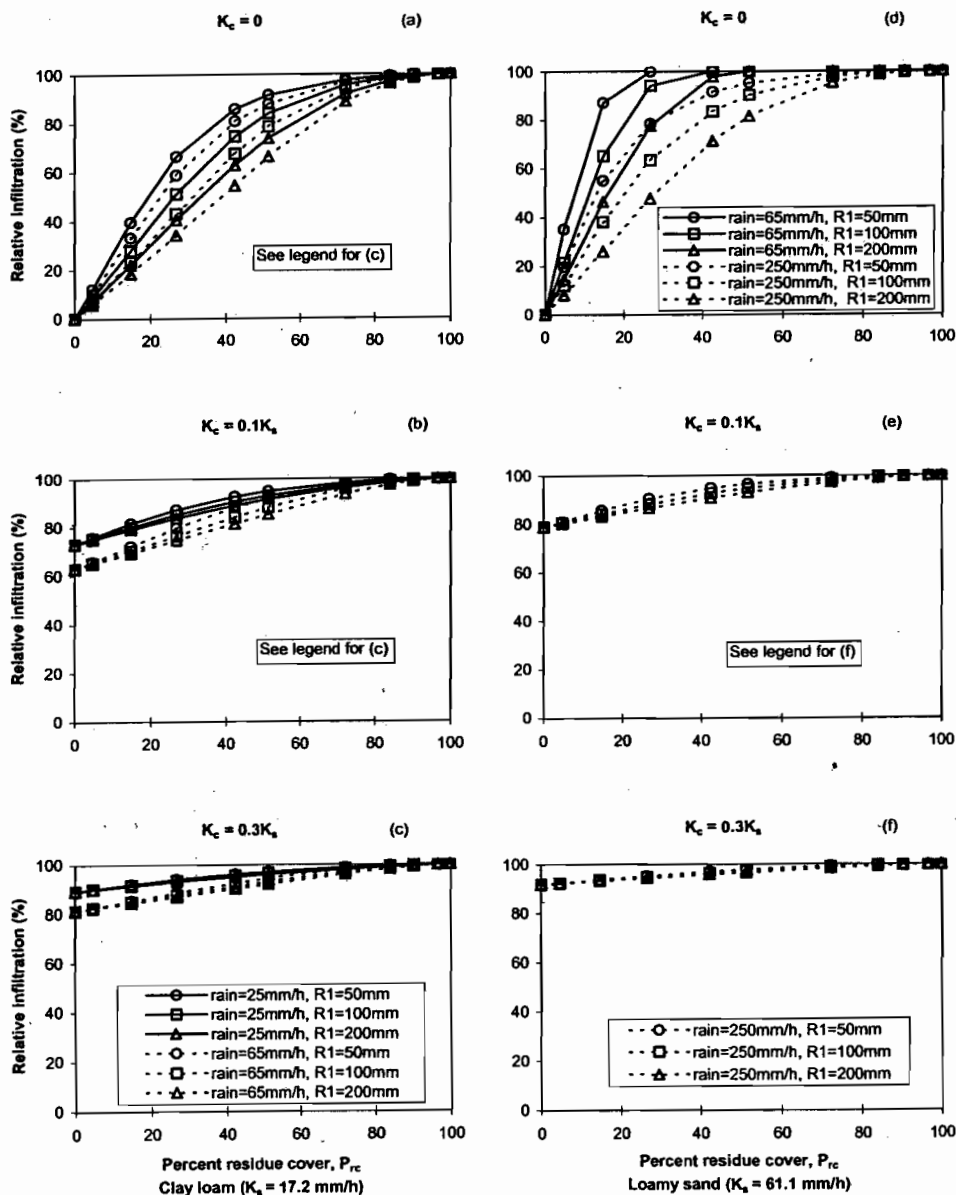


Fig. 3. Relative infiltration vs. percentage residue cover, P_{rc} , which is the percentage of residue-covered area of the total representative area (Type I). Relative infiltration is the cumulative infiltration at a value of P_{rc} divided by cumulative infiltration at $P_{rc} = 100\%$. For different values of P_{rc} , R_1 is kept constant.

surface sealing due to physical processes, and there is a limit of infiltration that is controlled by the soil itself.

Sensitivity of Residue-Cover Efficiency for Type I Residue Geometrical Distribution

Sensitivity of Residue-Cover Efficiency to the Way the Residue-Patch Size Changes

The simulated results of all other combinations (60 cases) for Type I residue geometrical distribution were summarized in Fig. 3 and 4. Each curve in the two figures represents the change of relative infiltration with the P_{rc} for a specific combination of soil type, K_s , residue-patch size, and rainfall intensity. Infiltration was normalized with the infiltration at a full residue cover ($P_{rc} =$

100%) to get the relative infiltration for easy comparison of residue-cover efficiency.

Figure 3 shows the simulated infiltration when P_{rc} was set to vary with the cylinder radius R_2 (a constant residue-patch radius R_1 for a specific curve). Figure 4 shows the simulated infiltration when P_{rc} was set to vary with residue-patch radius R_1 (with a constant cylinder radius R_2 for a specific curve). Comparing Fig. 3 and 4 shows that cases with constant cylinder radius R_2 had greater residue-cover efficiency (infiltration increased faster with P_{rc}) than cases with constant residue-patch radius R_1 . However, because of the similarity of the results, all further discussions will be based on the first scenario (when P_{rc} was set to vary with the cylinder radius R_2).

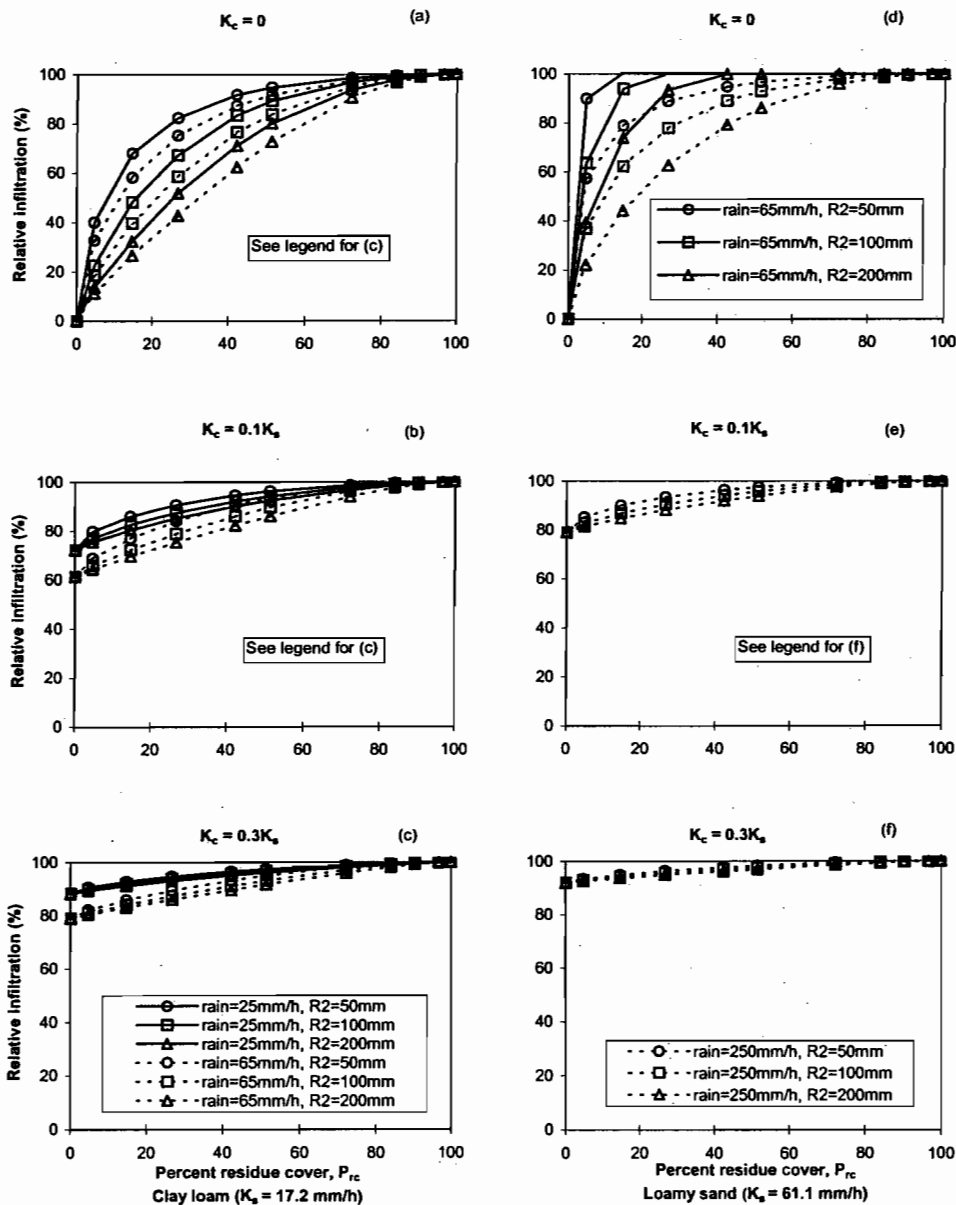


Fig. 4. Relative infiltration vs. percentage residue cover, P_{rc} , which is the percentage of residue-covered area of the total representative area (Type I). Relative infiltration is cumulative infiltration at a value of P_{rc} divided by cumulative infiltration at $P_{rc} = 100\%$. For different values of P_{rc} , R_2 is kept constant.

Sensitivity of Residue-Cover Efficiency to Soil Type

Figure 3 shows the relationships between the residue-cover efficiency and each of the four factors we selected earlier. Considering the soil type, the residue-cover efficiency for the loamy sand was greater than for the clay loam with $K_c = 0$, and similar with $K_c = 0.1K_s$ or $K_c = 0.3K_s$. The differences were caused not only by the soil type but also by the rainfall intensity values relative to the saturated hydraulic conductivity of the soil. With greater K or infiltration capacity in the residue-covered areas, the residue-cover efficiency was greater.

Sensitivity of Residue-Cover Efficiency to K_c

Considering the saturated hydraulic conductivity of the surface seal, the residue covers were more efficient with $K_c = 0$ than with $K_c = 0.1K_s$ or $K_c = 0.3K_s$ (see Fig. 3). This is obvious because with $K_c = 0$, residue cover increased the infiltration capacity from 0 to $>K_s$ in the residue-covered areas rather than from $0.1K_s$ or $0.3K_s$ to $>K_s$. The relationship was not linear. From $K_c = 0.1K_s$ to $K_c = 0.3K_s$, the residue-cover efficiency did not increase as much as from $K_c = 0$ to $K_c = 0.1K_s$.

Sensitivity of Residue-Cover Efficiency to Residue-Patch Size

Small residue patches had greater residue-cover efficiency than large residue patches at the same percent residue cover (see Fig. 3). With small residue-patch sizes and thus small surface-seal areas (at the same values of P_{rc}), water was more easily and evenly redistributed laterally in the soil after entering the residue-covered

areas, increasing the hydraulic gradient beneath small patches relative to large patches. Consequently, the infiltration capacity was greater for smaller residue patches. The decrease of infiltration capacity in the surface-sealed areas due to the redistributed water from residue-covered areas was much less because the original capacity was much less than in the residue-covered areas.

Sensitivity of Residue-Cover Efficiency to Rainfall Intensity

At high rainfall intensities, residue-cover efficiency was greater than at low rainfall intensities, except when $K_c = 0$ (Fig. 3). The increase of residue-cover efficiency with rainfall intensity was curvilinear and could reach an asymptotic limit. At $K_c = 0$, residue cover increased the infiltration capacity from zero to a number near the rainfall intensity more easily at low rainfall intensities than at high rainfall intensities. At $K_c = 0.1K_s$ or $K_c = 0.3K_s$, the infiltration capacity of surface seals was relatively high compared with low rainfall intensities and relatively low compared with high rainfall intensities. Therefore, the residue cover did not increase the infiltration as much at low rainfall intensities as at high rainfall intensities.

The Leveling-Off Values of P_{rc}

We used the infiltration without surface sealing (100% residue cover) as the maximum infiltration (100%). For different cases, the maximum infiltration changed. At 95% of the maximum infiltration, the value

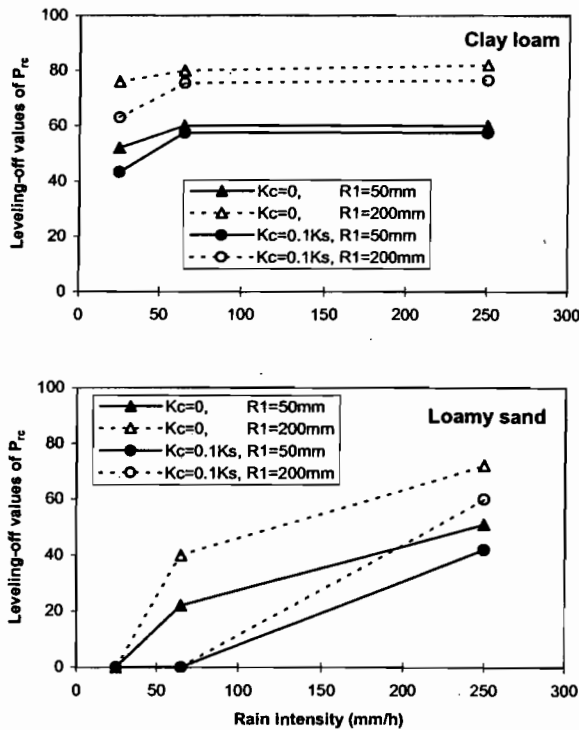


Fig. 5. Sensitivity of leveling-off value of P_{rc} to rainfall intensity (Type I). The value of P_{rc} at which the cumulative infiltration equals 95% of the cumulative infiltration at 100% P_{rc} is defined as the leveling-off value of P_{rc} .

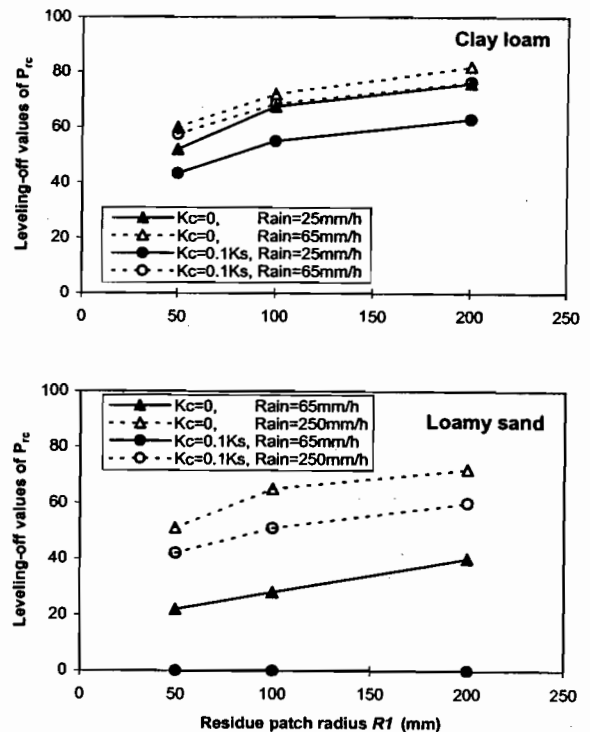


Fig. 6. Sensitivity of leveling-off value of P_{rc} to the residue-patch radius (Type I). The value of P_{rc} at which the cumulative infiltration equals 95% of the cumulative infiltration at 100% P_{rc} is defined as the leveling-off value of P_{rc} .

of P_{rc} was considered optimal (i.e., leveling off). Increasing P_{rc} value beyond 95% maximum infiltration was considered to not increase the infiltration efficiently, relative to the increase of residues. We examined how this optimal P_{rc} changed with rainfall intensity, residue size, the surface-seal saturated hydraulic conductivity, and soil type.

The leveling-off values of P_{rc} are plotted against rainfall intensity with different combinations of factors in Fig. 5. For loamy sand, the leveling-off values of P_{rc} increased from 0% (no residue-cover efficiency) at a rainfall intensity of 25 mm h⁻¹ to ≈57% at a rainfall intensity of 250 mm h⁻¹. It did not reach a limit at a rainfall intensity of 250 mm h⁻¹, but we assumed rainfall intensities >250 mm h⁻¹ were not practical. For clay loam, the leveling-off values of P_{rc} increased from ≈60% at a rainfall intensity of 25 mm h⁻¹ to ≈70% at a rainfall intensity of 250 mm h⁻¹. It reached a limit at a rainfall intensity of 65 mm h⁻¹.

The higher values of P_{rc} for clay loam soil, compared with the loamy sand soil, are due to lower hydraulic conductivities of clay loam soil near saturation, which result in less subsurface lateral flow from the residue-covered areas to sealed areas. Therefore, a clay loam soil requires greater residue cover to maintain an optimal infiltration rate. The optimal values of P_{rc} , of course, increase with rainfall intensity up to a limit.

Figure 6 shows the leveling-off values of P_{rc} against

the residue-patch size. The leveling-off values of P_{rc} increased curvilinearly with residue-patch size. At $R_1 = 200$ mm, the leveling-off values of P_{rc} for both soils did not reach a limit but increased less. The loamy sand had smaller leveling-off values of P_{rc} than the clay loam.

The optimal residue cover varies with conditions. It is necessary to know those conditions including rainfall intensity, soil types, and residue-patch sizes before determining the optimal residue cover. The results presented show the trends for the various conditions. The trends indicate that to obtain the maximum infiltration, (i) clay loam soils need more residue cover than loamy sand soils; (ii) more residue cover is needed when rainfall intensity is greater; (iii) more residue cover is needed when the soil can be surface sealed more easily; and (iv) it always helps to spread out residue cover uniformly.

Residue-Cover Efficiency for Type II Residue Geometrical Distribution

The simulated results for Type II distribution were similar to the results of Type I distribution. We omitted further discussions on Type II residue cover distribution.

One-Dimensional Solutions

The results of one-dimensional simulations are compared with those of the two-dimensional simulations in Fig. 7 for the residue-patch size of 50 mm. To better

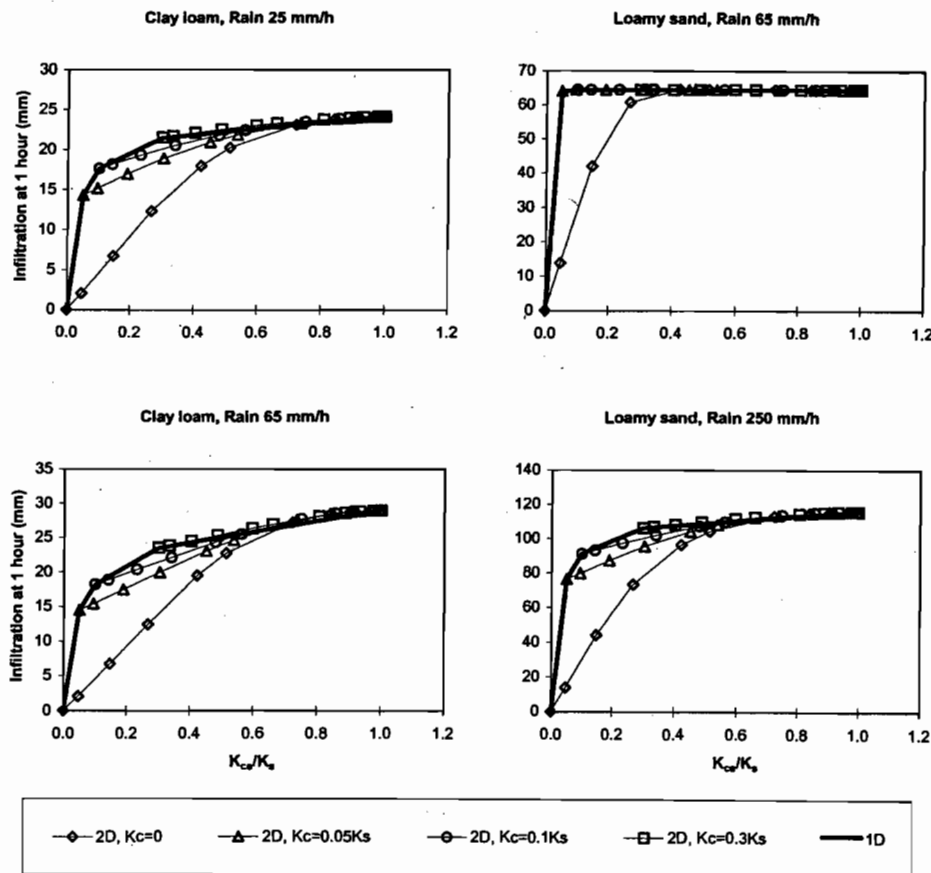


Fig. 7. One-dimensional solution with the effective surface sealing K_{cs} is compared with two-dimensional solutions with 4 degrees of surface sealing (Type I). Four combinations of soil textures and rainfall intensities were examined. For two-dimensional solutions, K_{cs}/K_s represents percentage residue cover.

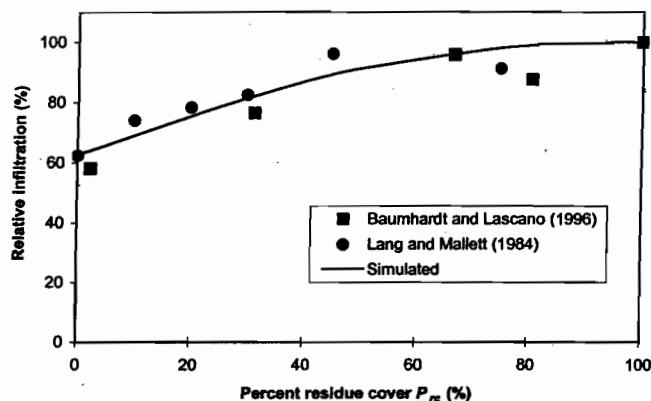


Fig. 8. Simulated results (Type I) are compared with field observations (after Baumhardt and Lascano, 1996; Lang and Mallett, 1984). The simulation input data are 65 mm h^{-1} rainfall intensity for a period of 1 h, 50-mm residue-patch radius, and $K_c = 0.1K_s$ for surface sealing.

understand the differences between the one-dimensional and two-dimensional methods, we also simulated four extra cases using $K_c = 0.05K_s$. If $K_c \geq 0.05K_s$, there were no significant differences between one-dimensional and two-dimensional results. When $K_c = 0$, the one-dimensional infiltration was much greater than the two-dimensional infiltration. For most practical conditions, $K_c \geq 0.05K_s$; it is seldom equal to zero. Therefore the one-dimensional method with Eq. [4] will give adequate estimates of the two-dimensional water infiltration and redistribution under partial residue-cover conditions.

Comparison with Two Independent Field Observations

Cumulative infiltration increased curvilinearly with P_{rc} in our results. This relationship agrees with the independent experimental observations literature (Baumhardt and Lascano, 1996; Lang and Mallett, 1984). In fact, our simulated results for the clay loam soil, with $K_c = 0.1K_s$, constant residue-patch size $R_2 = 50 \text{ mm}$, and rainfall intensity = 65 mm h^{-1} , agree with their observed data (Fig. 8). This soil type and the rainfall intensity are the same or nearly the same as those used in the above-mentioned studies. Soils of both experiments were clay loam. Their simulated rainfall intensities were 65 and 63.5 mm h^{-1} , respectively, for a period of 1 h. Values of the residue-patch size and the hydraulic conductivity of the surface sealing are within reasonable ranges of field conditions. Baumhardt and Lascano (1996) used residue mass as the quantity of residue cover. They found that the maximum cumulative infiltration, 49 mm, occurred when the residue amount increased to 3.6 Mg ha^{-1} . We used 3.6 Mg ha^{-1} as 100% residue cover and linear interpolation to convert the units of mass per area to units of percentage residue cover that we used in the simulations. We used 49 mm as the maximum cumulative infiltration to scale to relative infiltration. Lang and Mallett (1984) used percentage residue cover, which was used directly in Fig. 8. To find the maximum cumulative infiltration at 100% residue cover for scaling to relative infiltration, a polynomial curve that reaches its maximum at 100% residue cover

was fitted to the observed data of Lang and Mallett (1984), and the maximum cumulative infiltration was found to be 501 mm.

CONCLUSIONS

The efficiency of the crop-residue cover in increasing infiltration depends upon the soil type, hydraulic conductivity of the sealed surface, residue-patch size, and rainfall intensity. The residue-cover efficiency for the loamy sand soil was greater than for the clay loam soil. The residue-cover efficiency was greater when hydraulic conductivities of the surface seal were lower. The residue-cover efficiency was greater when residue-patch size was smaller but with the same percentage of residue cover. The residue-cover efficiency was greater when rainfall intensity was lower. In other words, more residue cover was needed to have the same percentage of infiltration increased for the clay loam soil, less surface sealing, larger residue-patch size, and greater rainfall intensity.

With the model for effective hydraulic conductivity of surface seal that we proposed, one-dimensional approaches can be used to simulate infiltration for soils that are partially and not severely surface sealed. If soils are severely surface sealed, the one-dimensional infiltration is much greater than the two-dimensional infiltration, making the present two-dimensional simulations necessary to realistically model field behavior for this extreme scenario.

The good agreements between the results of numerical simulations and the two independent experimental observations indicate that the numerical model that we proposed well represents the real system under complicated conditions. In the future, we will test (i) the residue geometrical distribution in strips to see its differences from a circular type, and (ii) layered soil profiles.

ACKNOWLEDGMENTS

The authors thank R. Louis Baumhardt, Greg Butters, and Liwang Ma for their helpful reviews before submission.

REFERENCES

- Ahuja, L.R. 1973. A numerical and similarity analysis of infiltration into surface-sealed soils. *Water Resour. Res.* 9:987-994.
- Ahuja, L.R. 1974. Applicability of the Green-Ampt approach to water infiltration through a surface seal. *Soil Sci.* 118:283-288.
- Ahuja, L.R. 1983. Modeling infiltration into surface-sealed soils by the Green-Ampt approach. *Soil Sci. Soc. Am. J.* 47:412-418.
- Ahuja, L.R., and D. Swartzendruber. 1992. Flow through surface-sealed soils: Analytical and numerical approaches. p. 93-122. *In* M.E. Sumner and B.A. Stewart (ed.) *Soil surface sealing: Chemical and physical processes*. Lewis Publishers, Boca Raton, FL.
- Baumhardt, R.L., and R.J. Lascano. 1996. Rain infiltration as affected by wheat residue amount and distribution in ridged tillage. *Soil Sci. Soc. Am. J.* 60:1908-1913.
- Baumhardt, R.L., M.J.M. Romkens, F.D. Whisler, and J.Y. Parlange. 1990. Modeling infiltration into a sealing soil. *Water Resour. Res.* 26:2497-2505.
- Benjamin, J.G., H.R. Havis, L.R. Ahuja, and C.V. Alonso. 1994. Leaching and water flow pattern in every-furrow and alternate-furrow irrigation. *Soil Sci. Soc. Am. J.* 58:1511-1517.
- Bruggeman, A.C., and S. Mostaghimi. 1991. Simulation of preferential flow and solute transport using an efficient finite element model. p. 244-255. *In* T.J. Gish and A. Shirmohammadi (ed.) *Preferential flow*. ASAE, St. Joseph, MI.

- Corey, A.T. 1994. Mechanics of immiscible fluids in porous media. Water Resources Publications, Highlands Ranch, CO.
- Duley, F.L. 1939. Surface factors affecting the rate of intake of water by soils. *Soil Sci. Soc. Am. Proc.* 4:60-64.
- Eigel, J.D., and I.D. Moore. 1983. Effect of rainfall energy on infiltration into a bare soil. p. 188-199. *In Advances in infiltration*. Proc. Natl. Conf. Advances in Infiltration, Chicago, IL. 12-13 Dec. 1983. ASAE, St. Joseph, MI.
- Ellison, W.D., and C.S. Slater. 1945. Factors that affect surface sealing and infiltration of exposed soil surface. *Agric. Eng.* 26:156-157.
- Lang, P.M., and J.B. Mallett. 1984. Effect of the amount of surface maize residue on infiltration and soil loss from a clay loam soil. *S. Afr. J. Plant Soil* 1:97-98.
- McIntyre, D.S. 1958. Permeability measurements of soil surface seals formed by raindrop impact. *Soil Sci.* 85:185-189.
- Morin, J., and Y. Benyamini. 1977. Rainfall infiltration into bare soils. *Water Resour. Res.* 13:813-817.
- Mualem, Y., and S. Assouline. 1989. Modeling soil seal as a nonuniform layer. *Water Resour. Res.* 25:2101-2108.
- Mualem, Y., S. Assouline, and D. Eitahan. 1993. Effect of rainfall-induced soil seals on soil water regime: Wetting processes. *Water Resour. Res.* 29:1651-1659.
- Philip, J.R. 1998. Infiltration into surface-sealed soils. *Water Resour. Res.* 34:1919-1927.
- Rawls, W.J., D.L. Brakensiek, J.R. Simanton, and K.D. Kohl. 1990. Development of a surface-seal factor for a Green Ampt model. *Trans. ASAE* 33:1224-1228.
- RZWQM Development Team: J.D. Hanson, L.R. Ahuja, M.D. Shaffer, K.W. Rojas, D.G. DeCoursey, H. Farahani, and K. Johnson. 1998. RZWQM: Simulating the effects of management on water quality and crop production. *Agric. Syst.* 57:161-195.
- Savabi, M.R., and D.E. Stott. 1994. Plant residue impact on rainfall interception. *Trans. ASAE.* 37:1093-1098.
- Simunek, J., T. Vogel, and M.Th. van Genuchten. 1994. The SWMS-2D code for simulating water flow and solute transport in two-dimensional variably saturated media. Version 1.2, Res. Rep. 132. U.S. Salinity Laboratory, USDA-ARS, Riverside, CA.
- Smith, R.E., C. Corradini, and F. Melone. 1999. A conceptual model for infiltration and redistribution in surface-sealed soils. *Water Resour. Res.* 35:1385-1393.
- Tackett, J.L., and R.W. Pearson. 1965. Some characteristics of soil surface seals formed by simulated rainfall. *Soil Sci.* 99:407-412.
- Unger, P.W., and B.A. Stewart. 1983. Soil management for efficient water use: An overview. p. 419-460. *In H.M. Taylor et al. (ed.) Limitations to efficient water use in crop production*. ASA, CSSA, and SSSA, Madison, WI.
- Van Genuchten, M.Th. 1980. A closed-form equation for predicting the hydraulic conductivity of unsaturated soils. *Soil Sci. Soc. Am. J.* 44:892-898.

Effect of Sediment Load on Soil Detachment and Deposition in Rills

G. H. Merten, M. A. Nearing,* and A. L. O. Borges

ABSTRACT

According to theory, the rate of detachment of soil particles in rills is reduced as a first-order function of the amount of sediment load in the flow. The first objective of this study was to determine if experimental results confirmed current detachment-transport coupling theory. The second objective was to investigate two hypothesized mechanisms responsible for any coupling effect observed: The first mechanism was that since turbulence is known to be a critical factor in detachment by flow, and since it is also known that sediment in water reduces turbulent intensity, it was suggested that sediment in flow reduces detachment via a correspondent reduction in turbulent intensities. This hypothesis was tested indirectly by adding a sediment load that was carried entirely in the suspended state. The second mechanism was that sediment covering the soil bed during the erosion process shields the soil from the forces of flow, thus reducing detachment. This hypothesis was tested by introducing bed-load sediment. Sediment loads exiting the rill and detachment and deposition along the rill were measured. Detachment was reduced and deposition increased as a linear function of the amount of sediment introduced into the flow. Results indicated that, in general, detachment did decrease according to current theory, but discrepancies in the erosional patterns were observed, which none of the current models explain. Both hypothesized mechanisms of reduction in detachment rates were apparently active in reducing detachment rates, though the shielding mechanism appeared to have a greater impact than did the mechanism associated with a reduction in turbulent intensity.

CONCENTRATED SURFACE WATER FLOW is capable of detaching and transporting sediments from the soil

G.H. Merten and A.L.O. Borges, Hydraulic Research Institute, Federal Univ. of Rio Grande do Sul, Box 15029, CEP 91501, Porto Alegre-RS, Brazil; M.A. Nearing, USDA-ARS National Soil Erosion Research Lab., Soil Bldg., Purdue Univ., West Lafayette, IN 47907-1196. Received 18 Jan. 2000. *Corresponding author (mnearing@purdue.edu).

Published in *Soil Sci. Soc. Am. J.* 65:861-868 (2001).

mass. The energy for these processes is provided, basically, by the weight of the mixture of water and sediment and the downslope gradient of the flow. Studies related to the mechanics of rill erosion have shown that rates of soil detachment are inversely dependent upon the magnitude of the sediment load at a given time and location on the soil surface (Meyer and Monke, 1965; Rice and Wilson, 1990; and Cochrane and Flanagan, 1996). The theoretical basis for this effect has been discussed by Foster and Meyer (1972) and Hairsine and Rose (1992a, 1992b).

Foster and Meyer (1972) (later presented in more detail by Foster, 1982) support the hypothesis that the flow possesses finite energy, which may be expended either to detach soil particles from the bulk soil mass or to transport previously detached sediments. Within this framework, it might be considered that the energy required to sustain movement of the sediment in transit, as well as to initiate movement of previously detached sediment particles resting on the bottom of the bed, is less than the energy necessary to detach new sediments from the soil mass. In this way, the energy is preferentially used for those processes related to the continuation of movement of the sediments. Any excess energy could then be available for detachment.

In the conceptual model of Foster and Meyer (1972), the flow energy available for detachment is calculated as the difference between sediment transport capacity minus the energy used for transport, represented by the sediment load in transit. Thus to estimate the rates of detachment it is essential to determine transport capacity.

A second theoretical model for the utilization of flow energy is that of Hairsine and Rose (1992a, 1992b). In this model, Hairsine and Rose propose that flow energy,